Mathematical studies of modulated differential scanning calorimetry–II. Kinetic and non-kinetic components

Jinan Cao*

CSIRO Division of Wool Technology, PO Box 21, Belmont, Vic. 3216, Australia

Abstract

Further to Part I of this study (Vol. 325, pp. 101–109), this article describes the mathematical expression of MDSC by taking melting, crystallization as well as the temperature dependence of the heat capacity of a sample into consideration. A numerical method has been established and found to be suitable for the simulation of MDSC thermograms. It is found that a non-kinetic thermal event results in changes in the amplitude of heat flow of the thermogram of MDSC, but a kinetic thermal event causes no change in the amplitude of heat flow. A quantitative separation of the kinetic and non-kinetic components is, however, problematic since there is no linear relationship between the amplitude and the thermal parameters of a sample. © 1999 Published by Elsevier Science B.V. All rights reserved.

Keywords: Temperature modulation; DSC; Reversing component; Kinetics; Numerical simulation

1. Introduction

It has been claimed that the ability to disentangle reversing and non-reversing components of a thermal event is the most important advantage of MDSC over the conventional DSC [1–7]. This has been achieved by subtracting the heat capacity component, determined by the amplitude of heat flow, from the total averaged or underlying heat flow, as proposed by Reading et al. and Wunderlich et al. [1–7]. A quenched polyethylene terephthalat (PET) has been used for demonstration in most of the cases. According to these results, the crystallization of a quenched PET is a non-reversing thermal event, and the melting of PET is found to be a reversing thermal event under the experimental conditions adopted in those studies.

However, from those published MDSC data, it appears that the separation of the reversing and non-reversing components for the melting of PET is dependent on the modulation conditions [1–7]. The physical interpretation of the "reversing" and "non-reversing" seems to be inconsistent from the formal logic point of view. If why the melting is considered to be "reversing" is because the PET sample is crystallizing while its melting under the specific experimental conditions employed [1–7]; why is not the crystallization thought to be "reversing" since the sample is melting while its crystallization? Indeed the meaning of "reversing" or "non-reversing" is fairly ambiguous. In particular, as shown in Part I of this study [8], the amplitude of heat flow is a nonlinear function of a number of factors, its quantitative

*Tel.: +61-3-5246-4000; fax: +61-3-5246-4057; e-mail: jinan.cao@dwt.csiro.au

determination is not conveniently practicable. These facts raise the question whether the extracted reversing and non-reversing components do indeed reflect the intrinsic nature of the sample tested.

The basis of MDSC can be understood through a detailed mathematical analysis of the processes. It will be shown below that kinetic and non-kinetic thermal events in MDSC can be described using a differential equation, and how the equation can be numerically solved.

It is found that a non-kinetic thermal event results in changes in the amplitude of heat flow of the thermogram of MDSC, but a kinetic thermal event causes no change in the amplitude of heat flow. A quantitative separation of the kinetic and non-kinetic components is, however, problematic since there is no linear relationship between the amplitude and the thermal properties of a sample.

2. Generalized differential equation of MDSC

Consider a sample experiencing heat generation (in this article, heat adsorption is considered to be negative heat generation) due to physico-chemical transition or reaction. The equation of energy balance for the sample may be written as

$$\frac{dT_s(t)}{dt} = \frac{1}{C_{ps}[T_s(t)]} \left(\frac{dQ}{dt} + \frac{dQ'}{dt} \right), \tag{1}$$

where dQ and dQ' are the heat adsorbed by the sample from the heating block and the heat generated in the sample due to a physico-chemical change involving heat respectively. Note that the heat capacity of the sample is no long a constant in this article.

The equations for the heating program and Newton's law of cooling are still the same as those shown in Part I of this study (Eqs. (1) and (3)). A reference shall experience no physico-chemical change during a thermal analysis, so Eq. (7) in Part I is applicable for the reference without any modification.

Combining Eqs. (1), (3) of part I and (1) leads to

$$\frac{dT_s(t)}{dt} = \frac{\lambda}{C_{ps}[T_s(t)]}$$
$$\times \left[T_{b0} + qt + A_b \sin \omega t - T_s(t) + \frac{dQ'}{dt} \right]. \tag{2}$$

Eq. (2) is the generalized form of the governing equation of MDSC.

The form of dQ' resulting from a physico-chemical is important as it determines the structure of the solution of the differential equation. For a non-kinetic thermal event, defined as a thermal event that occurs as soon as the sample reaches a certain temperature without time delay, compared with the time scale of an MDSC experiment in this article. dQ' can be written in the form:

$$dQ' = f[T_s(t)] dT_s \tag{3}$$

where, f represents an arbitrary function of the temperature of the sample, which in turn is a function of time, t.

Eqs. (2) and (3) can be combined and rearranged

$$\frac{dT_s(t)}{dt} = \frac{\lambda}{C_{ps} - \lambda f} [T_{b0} + qt + A_b \sin \omega t - T_s(t)]. \tag{4}$$

Eq. (4) shows that a non-kinetic physico-chemical change should have the equivalent effect as the temperature dependence of the heat capacity of a sample. Thus an identical MDSC thermogram is expected.

On the other hand, for a kinetic thermal event, dQ' would have the form

$$dQ' = g[T_s(t), t] dT. \tag{5}$$

Eq. (2) becomes

$$\frac{dT_s(t)}{dt} = \frac{\lambda}{C_{ps}} [T_{b0} + qt + A_b \sin \omega t - T_s(t) + g(t, T_s)]. \tag{6}$$

Eqs. (4) and (6) are the general forms of the differential equations of MDSC for non-kinetic and kinetic thermal events. In the following, detailed mathematical expressions for the non-kinetic and kinitic processes using crystallization and melting of a polymer as examples will be presented.

2.1. Mathematical expression of a non-kinetic example

Crystal melting is a typical example of non-kinetic physical transition. Whereas crystallization of polymers is a kinetic process, melting is usually understood to be temperature only determined. This is to say
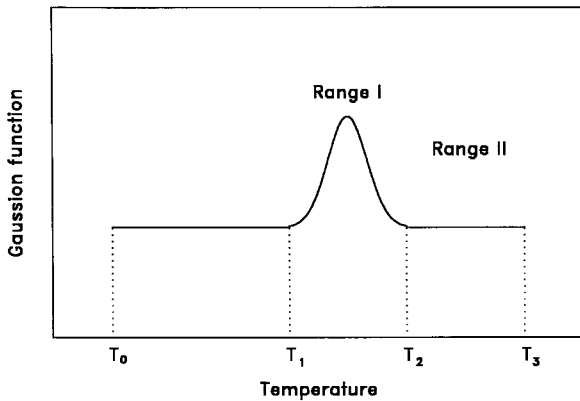
Fig. 1. A Gaussian function of temperature.

that a melting process completes as soon as the temperature of a crystal reaches its melting point. A broad melting peak is usually observed for a polymer. This is caused by the factors such as a broad crystallite size distribution. Assuming a sample with melting peak distribution as a Gaussian function shown in Fig. 1, one obtains the expression for the melting heat

$$\mathrm{d}Q' = \Delta H_\mathrm{m}^0 \, m G(T_\mathrm{s}(t)) \, \mathrm{d}T_\mathrm{s}, \tag{7}$$

where ΔH_m^0, m represent the melting enthalpy and the mass of the sample; G is the Gaussian function, which is written as

$$G(T_\mathrm{s}(t)) = G_0 \exp\left(-\frac{4\ln 2 [T_\mathrm{s}(t) - T_\mathrm{max}]}{\mu_\mathrm{m}^2}\right) \tag{8}$$

where, G_0, T_max and μ_m denote the pre-exponential factor, the peak temperature and the width at half-height of the Gaussian curve [9–11].

Now consider the specific heat capacity of a sample showing temperature dependence in such a manner as illustrated in Fig. 1. This assumption may not reflect physical reality. It is an imaginary sample for the mathematical convenience. The mathematical description using the Gaussian function is

$$C_\mathrm{ps} = C_\mathrm{ps}^0 \left[1 + A_\mathrm{cp} \exp\left(-\frac{4\ln 2 [T_\mathrm{s}(t) - T_\mathrm{max}]}{\mu_\mathrm{cp}^2}\right)\right] \tag{9}$$

where, A_cp, T_max and μ_cp denote the pre-exponential factor, the temperature at which the specific heat

capacity of the sample reaches its maximum and the width at half-height of the Gaussian curve. C_ps^0 is a constant equal to the heat capacity of the sample over the temperature Range 0 and Range II.

Comparing Eqs. (4), (7), (8) and (9), one can easily understand that a non-kinetic thermal event is mathematically equivalent with the temperature dependence of the heat capacity of a sample despite they have different physical meanings. Thus identical thermograms of MDSC are expected. In Section 3, only will the temperature dependence be addressed.

2.2. Mathematical expression of a kinetic example

Crystallization of a polymer is a typical example of kinetic process. Considering the latent heat of crystallization, one obtains

$$\mathrm{d}Q' = \Delta H_\mathrm{m}^0 \, m \, \mathrm{d}x_\mathrm{c}(t), \tag{10}$$

where x_c represents the crystallinity of the sample. Under the isokinetic assumption, the crystallinity can be expressed in the following generalized equation for a non-isothermal crystallization [9–11]

$$x_\mathrm{c}(t) = 1 - \exp\left[-\left(\int_0^t K[T_\mathrm{s}(\tau)] \, \mathrm{d}\tau\right)^n\right], \tag{11}$$

where, n is the Avrami crystallization index. The symbol τ denotes the time variable of the integrand. K is a crystallization rate function, which can be written by using the Gaussian function

$$K[T_\mathrm{s}(t)] = A_K \exp\left(-\frac{4\ln 2 \, [T_\mathrm{s}(t) - T_\mathrm{max}]^2}{\mu_K^2}\right), \tag{12}$$

where, A_K, T_max and μ_K denote the pre-exponential factor, the temperature at which the crystallization rate function of the sample reaches maximum and the width at half-height of the Gaussian curve.

Combining Eqs. (10)–(12) leads to

$$\mathrm{d}Q' = \Delta H_\mathrm{m}^0 \, m \, n \, K\,[T_\mathrm{s}(t)] \exp \\ \left[-\left(\int_0^t K\,[T_\mathrm{s}(\tau)] \, \mathrm{d}\tau\right)^n\right] \left(\int_0^t K\,[T_\mathrm{s}(\tau) \, \mathrm{d}\tau\right)^{n-1} \mathrm{d}t. \tag{13}$$

Eq. (13) is the mathematical expression for the heat generation of crystallization of a polymer.

3. Numerical method for the differential equation

Differential equation (2) is in general not analytically solvable as C_{ps} is no long a constant and dQ'/dt has a complicated form. However, it can always be numerically solved with the aid of a computer by replacing the differential equation using a difference equation. A Runge–Kutta method with fourth order accuracy [12] has been employed in this study.

To facilitate computation using the Runge–Kutta method, Eq. (2) is rewritten in the form

$$\frac{dT_s(t)}{dt} = h(t, T_s), \tag{14}$$

where, $h(t, T_S)$ means a function of time, t, and temperature, T_S. The initial condition is given as:

$$\text{when} \quad t = t_1, \quad T(t_1) = T_1. \tag{15}$$

When the time increment, Δt, is sufficiently small, one can obtain the temperature at time, $(j+1)\Delta t$, from the temperature at time, $j\Delta t$ (where $j=0, 1, 2, 3, \ldots$), according to the Runge–Kutta method.

$$T[(j+1)\Delta t] = T(j\Delta t) + \frac{k_0 + 2k_1 + 2k_2 + k_3}{6}, \tag{16}$$

where

$$k_0 = \Delta t \, h \, [j\Delta t, T_s(j\Delta t)], \tag{17}$$

$$k_1 = \Delta t \, h \left[j\Delta t + \frac{\Delta t}{2}, T_s(j\Delta t) + k_0/2 \right], \tag{18}$$

$$k_2 = \Delta t \, h \left[j\Delta t + \frac{\Delta t}{2}, T_s(j\Delta t) + k_1/2 \right], \tag{19}$$

$$k_3 = \Delta t \, h \left[j\Delta t + \frac{\Delta t}{2}, T_s(j\Delta t) + k_2/2 \right]. \tag{20}$$

To minimize the discretization error so that the numerical solution has sufficient accuracy and precision, a very small time increment is necessary. It is found that this can be achieved when Δt
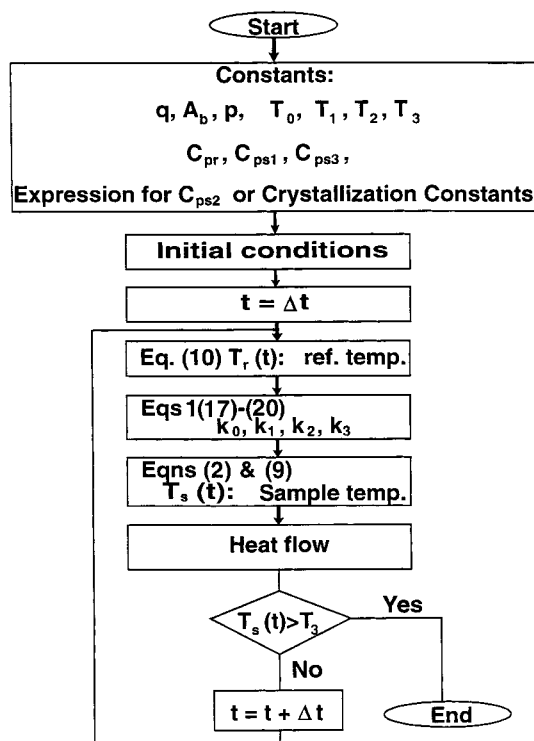

Fig. 2. Flow chart of the simulation program using the Runge–Kutta method for MDSC thermograms (Eq. (10): part I).

approaches 1/60 000 of the whole duration of an MDSC experiment. On the other hand, the round-off error can be minimized by adopting double precision computation. Fig. 2 shows the flow chart of the computer program.

4. Results and discussion

To demonstrate the accuracy and stability of the numerical simulation, the Runge–Kutta method has been used to solve the analytically solvable differential equation (6) of part I. Fig. 3 shows the results, where all the conditions are the same as those used for Fig. 7 of part I except a smaller heat capacity of the reference, C_{pr}. Also displayed in Fig. 3 are three normal DSC curves with heating rates of 4°C/min, 5°C/min and 6°C/min, respectively. The thermograms obtained using the numerical method and analytical solution are essentially indistinguishable, indicating the numerical method is highly accurate and stable.
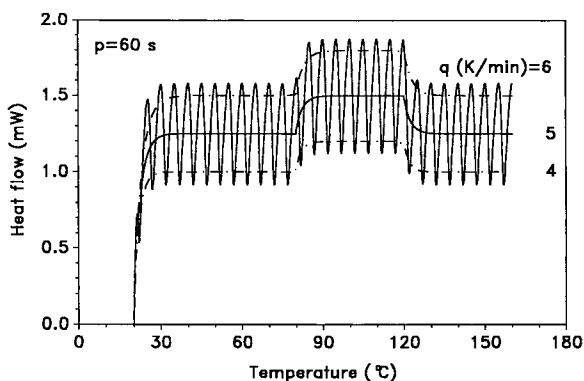
Fig. 3. Comparison between the numerical solution using the Runge–Kutta method and the analytical solution shown in Fig. 7 of part I.

It is also clear from Fig. 7 of part I and Fig. 3 that the amplitude of the heat flow varies as the heat capacity of the reference changes, although the difference in heat capacities between the sample and reference, and other conditions are kept constant, suggesting that a quantitative determination of the heat capacity of a sample using the amplitude of the heat flow will be difficult.

Figs. 4 and 5 show the simulated thermograms with and without modulation for a sample whose heat capacity is a Gaussian function of temperature over Range I shown in Fig. 1. The simulation conditions employed are listed in Table 1. The peak of endotherm or exotherm of the thermograms has shifted to a higher
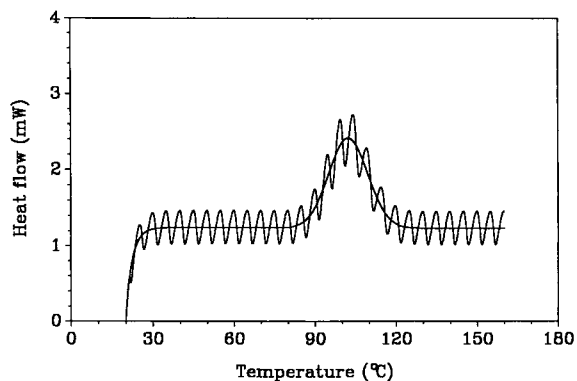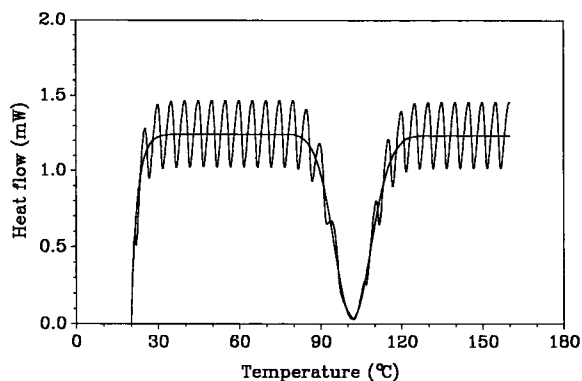

Fig. 5. Numerically simulated thermograms of both MDSC and normal DSC for a sample showing temperature dependence as a Gaussian function (decreasing) in its heat capacity over the temperature Range I.

temperature by about $2°C$ from the peak temperature of the Gaussian function defined in Fig. 1 and Table 1. This shift is a result of the transient effect of DSC or MDSC since C_{ps} varies continuously during the temperature Range I. Qualitatively, the amplitude of heat flow does increase with increasing the heat capacity of the sample.

The amplitude of heat flow over the temperature Range I becomes rather difficult to determine as it is superimposed on an steep endotherm or exotherm. This difficulty, however, can be overcome by subtracting the thermogram of normal DSC from that of MDSC, as illustrated in Fig. 8 of part I. Fig. 6 shows the results. Although the amplitude of heat flow does

Fig. 4. Numerically simulated thermograms of both MDSC and normal DSC for a sample showing temperature dependence as a Gaussian function (increasing) in its heat capacity over the temperature Range I.
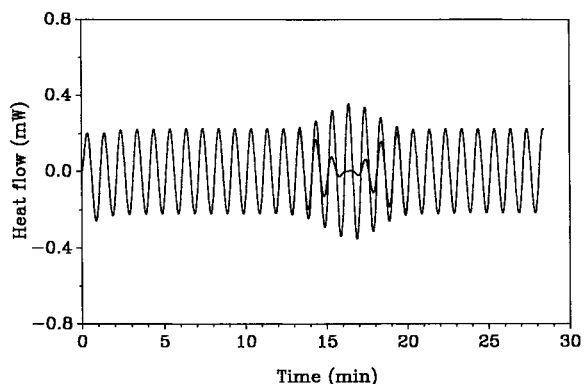

Fig. 6. Amplitude of heat flow changes for a non-kinetic thermal event.

Table 1
Numerical parameters employed for the simulations of Figs. 4, 5 and 7

Figure	$\lambda (J/K_s)$	p (s), A_b $(°C)$, q $(°C)$	C_{pr} (J/K)	C_{ps} (J/K) 20–80°C	C_{ps} (J/K) Range I 80–120°C	C_{ps} (J/K) Range II 120–160°C
4	0.002	60, 1, 5	0.030	0.045	$A_{cp}=0.015$ $T_{max}=100°C$ $\mu_{cp}^2 = 250$	0.045
5	0.002	60, 1, 5	0.030	0.045	As above except $A_{cp}=-0.015$	0.045
7	0.002	60, 1, 5	0.040	0.055	$A_K=0.005$, $T_{max}=100°C$, $\mu K^2=250$, $n=4$ $\Delta H_m^0=30$ (J/K), $m=10$ mg	0.055

increase or decrease with changing the heat capacity of the sample, its increment or decrement is non-linear. It is therefore possible that the reported "non-reversing" component for PET [1–7] purely results from this non-linear effect.

A kinetic thermal even e.g., crystallization on the amplitude of heat flow has also been simulated and the results are displayed in Fig. 7. The peak of the crystallization exotherm has shifted from the peak temperature where the crystallization rate constant, K, reaches its maximum, by around 6°C. This is caused by the transient effect as well as the kinetic effect. Over the peak area, the amplitude of heat flow becomes difficult to determine. Thus the thermogram of conventional DSC has been subtracted from that of MDSC, Fig. 8 shows the result. Clearly the amplitude of heat flow remains unchanged during the crystallization process, indicating that the amplitude of heat flow of an MDSC thermogram keeps constant during a kinetic process.

Fig. 9 shows the simulation results for the crystallinity development during the heating processes shown in Fig. 7. The crystallinity of the sample
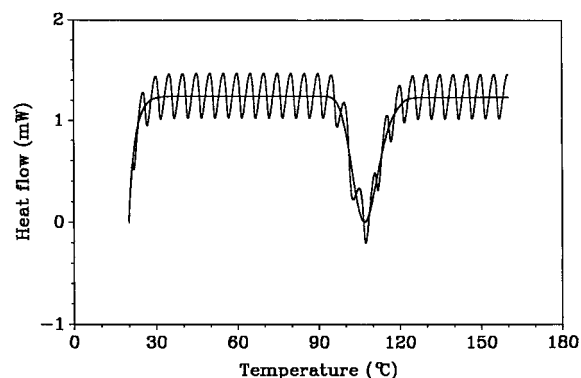
increases with temperature monotonically in both cases although there are more waves resulting from the modulation in the curve of MDSC. At the heating rate of 3°C/min the sample has fully crystallized during the heating process.

A major reason for people to believe that MDSC can disentangle reversing and non-reversing components of a thermogram is the sinusoidal modulation superimposed on the linear heating ramp. This sinusoidal modulation has appeared to invite people to consider that this component can be related to reversing component of a thermal event despite the overall heating rate does not show alternative change of heating and cooling.

However, according to the theory of Fourier series, a linearly increased temperature can be written as the superposition of a series of trigonometric functions as well [12]

$$qt = 2\sin(qt) - \sin(2qt) + \frac{2}{3}\sin(3qt)$$
$$- \frac{1}{2}\sin(4qt) + \cdots \qquad (21)$$

Fig. 7. Numerically simulated thermograms of both MDSC and normal DSC for a sample experiencing crystallization over the temperature Range I.
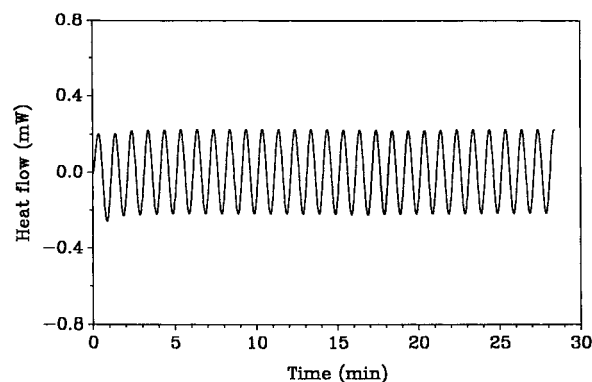

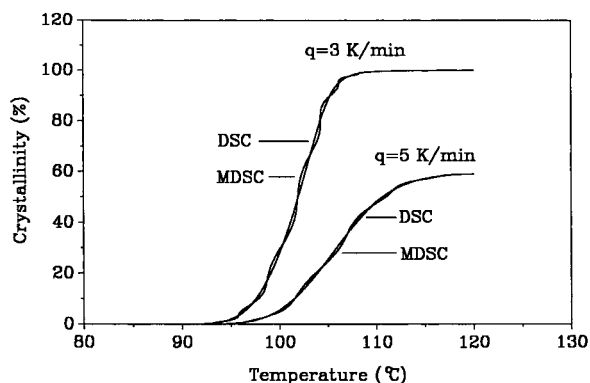Fig. 8. Amplitude of heat flow shows no change over a kinetic thermal event.

Fig. 9. Crystallinity development during heating in a DSC and MDSC cells.

No reversing and non-reversing discussion has been considered to be necessary for the above equation since the overall heating rate is a linear ramp. This important aspect has been obviously disregarded.

5. Conclusions

The complete mathematical description of MDSC, incorporation melting, crystallization and the temperature dependence of the heat capacity of a sample into consideration, has been established. A Runge–Kutta method with fourth accuracy has been found to be suitable to solve the differential equation. It is found that a non-kinetic thermal event results in changes in the amplitude of heat flow of the thermogram of MDSC, but a kinetic thermal event has no effect in changing the amplitude of heat flow. How-ever, a quantitative separation of the kinetic and non-kinetic components from an MDSC thermogram is not straightforward since there is no linear relationship between the amplitude and the thermal parameters of the sample.

Appendix

The numerical computations were performed using an IBM personal computer of 33 MHz equipped with a 487 co-processor. The most complicated numerical simulation required less than 25 min.

References

[1] M. Reading, D. Elliot, V.L. Hill, Proceedings of the Ninth ICTA Meeting, Hatfield, UK, August 1992.
[2] M. Reading, D. Elliot, V.L. Hill, J. Therm. Anal. 40 (1993) 949–955.
[3] P.S. Gill, S.R. Saurbrunn, M. Reading, Proceedings of the Ninth ICTA Meeting, Hatfield, UK, August 1992.
[4] P.S. Gill, S.R. Saurbrunn, M. Reading, J. Therm. Anal. 40 (1993) 931–939.
[5] M. Reading, Trends Polym. Sci. 8(1) (1993) 248–253.
[6] B. Wunderlich, Y. Jin, A. Boller, Thermochim. Acta 238 (1994) 277–293.
[7] M. Reading, A. Luget, R. Wilson, Thermochim. Acta 238 (1994) 295–307.
[8] J. Cao, Thermochimica Acta 325 (1999) 101–109.
[9] J. Cao, Polymer 33 (1992) 3520–3521.
[10] J. Cao, J. Appl. Polym. Sci. 49 (1993) 1759–1768.
[11] J. Cao, T. Kikutani, A. Takaku, J. Shimizu, J. Appl. Polym. Sci. 37 (1989) 2683–2697.
[12] G.A. Korn, T.M. Horn, Mathematical Handbook for Scientists and Engineers, 2nd ed., McGraw-Hill, New York, 1968.